IEEE Photonics Journal
An IEEE Photonics Society Publication

Open Access

Phase Retrieval Utilizing Particle Swarm Optimization

Volume 10, Number 1, February 2018

Li-Jing Li
Teng-Fei Liu
Ming-Jie Sun, ***Member, IEEE***

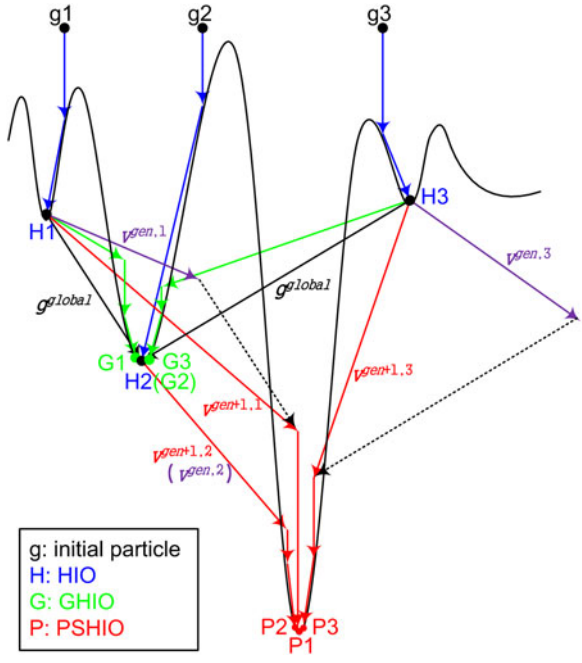

DOI: 10.1109/JPHOT.2017.2784541
1943-0655 © 2017 IEEE

Phase Retrieval Utilizing Particle Swarm Optimization

Li-Jing Li, Teng-Fei Liu, and Ming-Jie Sun, *Member, IEEE*

Department of Opto-Electronic Engineering, Beihang University, Beijing 100191, China

DOI:10.1109/JPHOT.2017.2784541

Manuscript received October 18, 2017; revised December 6, 2017; accepted December 13, 2017. Date of publication December 21, 2017; date of current version January 3, 2018. This work was supported in part by the National Natural Science Foundation of China under Grants 61675016 and 61307021, and in part by the Beijing Natural Science Foundation under Grant 4172039. Corresponding author: Ming-Jie Sun (e-mail: mingjie.sun@buaa.edu.cn).

Abstract: Phase retrieval is an important tool for image recovery techniques based on Fourier spectrum. Different iterative algorithms have been developed to retrieve phase information. However, due to the nonconvex feature of the phase optimization problem, it remains a challenge to globally obtain the optimal phase information. In this work, we proposed an iterative algorithm to retrieve the global optimal phase information by adopting particle swarm optimization technique to the hybrid input–output scheme. By escaping the local minima using stochastic perturbations and information exchange among particles' local solutions, the proposed scheme increases the possibility of reaching the global minimum in phase retrieval optimization. In the numerical simulations, the images reconstructed by the proposed scheme have an averaged mean-square error of 0.0055, which is, respectively, 43.88% and 36.78% smaller than those of the images reconstructed by hybrid input–output and guided hybrid input–output schemes. The feasibility of the proposed scheme was demonstrated by the results from actual experiments, which showed an agreement with the simulation. The proposed scheme is statistically capable of obtaining accurate phase information, and, therefore, can be applied to Fourier spectrum based image recovery techniques.

Index Terms: Phase retrieval, image reconstruction, particle swarm optimization.

1. Introduction

Phase retrieval and image reconstruction [1]–[14] play an important role in many imaging techniques. Some of them [7], [8], [11], [12] obtain Fourier complex amplitudes of a scene and use inversed Fourier transform to reconstruct the image of the scene. More often than not, the phase information of the Fourier complex amplitudes are lost during the measurements, because most detectors are light intensity sensitive only. It is difficult to reconstruct the image directly with inversed Fourier transform using the amplitude information along. In order to retrieve the phase information, many iterative phase retrieval algorithms [2], [15]–[22] have been developed. Fienup's hybrid input output (HIO) algorithm [16] is one of the most widely used scheme, which manages to obtain an approximation of the original phase information by minimizing an error function through iterations between space domain and Fourier domain. HIO is a big progress in Fourier magnitudes phase retrieval, however, one of its limitations is that HIO is only efficient in seeking out a local minimum, and therefore the solutions can be easily trapped to a local minimum in phase retrieval due to the non-convex feature of Fourier magnitudes. The accuracy of the retrieved phase is profoundly relied on the position of the initial particle [23], i.e., a two-dimensional random intensity distribution, which

is randomly generated. In order to increase the possibility of achieving global minima, HIO often performs multiple independent reconstruction procedures with different random initial particles [24]. However, different initial particles produce diverse results, and if no prior information of the object is provided, then an awkward situation of deciding the optimal image among these diverse results will be posed.

In order to improve the consistency of reconstructed images, Chen et al. proposed guided hybrid input-output (GHIO) algorithm [25] by combining guiding searching with HIO. GHIO starts a certain number of iterations with several random initial particles in parallel as the first generation. The reconstructed image with the lowest value of an error function in the first generation is then selected to be multiplied to other reconstructed images, and the square roots of the products, or the geometric averages, are functioned as the initial particle for the second generation. This procedure is repeated so that all outcomes are converged to a certain minimum [26]. GHIO addresses the problem of inconsistencies occurring in multiple independent reconstructions by converging solutions to the optimal one among these reconstructions. However, its ability to reach the global minimum is still limited because the iteration procedure is guided by the best solution among the initial particles.

Aiming to increase the possibility of obtaining the global optimal solution in phase retrieval, here we proposed a global optimization approach through searching the phase solution space by adopting the particle swarm optimization (PSO) to reach the global optimal solution in HIO scheme. Originally introduced by Kennedy and Eberhart [27], PSO is a stochastic evolutionary optimization technique which searches for a global minimum by imitating social behavior of organisms. Our PSO adopted HIO scheme, hereafter referred as PSHIO, can escape from local minima which are determined by the random initial particles, and increase the possibility of seeking out the global minimum by stochastic perturbations and information exchange among particles' local solutions. Results from both numerical simulations and actual experiments demonstrated that compared to HIO and GHIO, the proposed PSHIO scheme retrieved more accurate phase and consequently reconstructed images with better qualities.

2. PSHIO Reconstruction Protocol

Fienup's HIO algorithm is widely used for Fourier magnitudes phase retrieval. The algorithm consists of the following four steps:

1) Assuming that the object intensity distribution $g(m, n)$ is nonnegative, iteration is executed between Fourier-domain and object-domain. The first estimation of the object $g_0(m, n)$ is generated randomly, and for the kth iteration, the Fourier pattern $G_k(u, v)$ is generated by Fourier transform of the reconstructed image $g_k(m, n)$,

$$G_k(u, v) = |G_k(u, v)| \exp[i\phi_k(u, v)] = \mathcal{F}\{g_k(m, n)\} \tag{1}$$

where $\mathcal{F}$ stands for the two-dimensional Fourier transform.

2) A new Fourier pattern $G'_k(u, v)$ is formed by replacing the magnitudes with the experimental data $|F(u, v)|$,

$$G'_k(u, v) = \left|F(u, v)\right| \exp\left[i\phi_k(u, v)\right] \tag{2}$$

3) For the next step, $G'_k(u, v)$ is then inversed Fourier transformed to generate a middle reconstructed image $g'_k(m, n)$,

$$g'_k(m, n) = \mathcal{F}^{-1}\left\{G'_k(u, v)\right\} \tag{3}$$

where $\mathcal{F}^{-1}$ stands for the inversed Fourier transform.

4) The $(k+1)$th reconstructed image $g_{k+1}(m, n)$ can be calculated as,

$$g_{k+1}(m, n) = \begin{cases} g'_k(m, n) & (m, n) \in S \cap g'_k(m, n) \geq 0 \\ g_k(m, n) - \beta g'_k(m, n) & others \end{cases} \tag{4}$$

where S denotes finite constraint called support region and β is a feedback parameter [16].

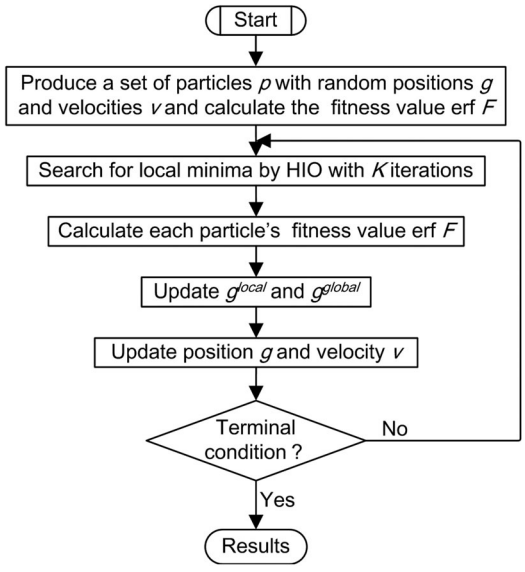

Fig. 1. A flowchart of PSHIO procedure.

The four steps consist one iteration of HIO algorithm, which is then repeated until the reconstructed image $g_k(m, n)$ converges in most cases.

PSO is a stochastic global optimization approach to solve the problem of local minima. It employs a number of random initial particles as a group. Each particle with two attributes position and velocity, is treated as a potential solution of the problem. After initialization, it drives these particles around in searching space by using a fitness function. During the solving process, each particle's motion is not only influenced by its individual best known position, but by the group's best known position which has been observed in searching space. All these particles are evolved by stochastic perturbations and position information exchange among themselves through generations [28]. This is expected to drive the particles toward the global optimal solution.

PSO can be applied to Fourier magnitudes phase retrieval since it does not require gradient feature of the problem being optimized [29]. Assuming that each particle represents a solution of object's image, we combine the PSO technique with HIO algorithm to form our proposed PSHIO algorithm as following steps (see Fig. 1).

1) A set of estimate particles $g^i (i = 1, 2, \ldots, p)$ of the object's image is produced. The position g^i and the velocity v^i of particle i are initialized with random values,

$$g_0^{gen,i} = g_0^{gen,i}(m, n) \quad i = 1, 2, \ldots, p \tag{5}$$

$$v_0^{gen,i} = v_0^{gen,i}(m, n) \quad i = 1, 2, \ldots, p \tag{6}$$

where gen denotes the gen th generation and $gen = 1$ is this initial particle.

According to [25], the fitness function erf F of each particle can be defined as following,

$$\text{erf } F = \frac{\sum_{(u,v)\in D} \left| |F(u, v)| - \left| \mathcal{F}\left\{ g_k^{gen,i}(m, n) \right\} \right| \right|}{\sum_{(u,v)\in D} |F(u, v)|} \tag{7}$$

where D represents the whole searching space. erf F evaluates the error between Fourier magnitude of the current particle and the experimental data $|F(u, v)|$, with the assumption that the smaller erf F is, the better quality the reconstructed image of the current particle has. Each initial particle is treated as the individual best known position $g^{local,i} (i = 1, 2, \ldots, p)$ and the particle with the smallest erf F is treated as the group's best known position g^{global} among these particles.

2) Each particle is run with K iterations.
3) Each particle's fitness value erf F can be calculated.
4) Each particle's individual best known position and the group's best known position for next generation can be updated as followings,

$$g^{local,i} = \begin{cases} g_K^{gen,i}, & \text{erf } F\left(g_K^{gen,i}\right) \leq \text{erf } F\left(g^{local,i}\right) \\ g_K^{local,i}, & \text{erf } F\left(g_K^{gen,i}\right) \geq \text{erf } F\left(g^{local,i}\right) \end{cases} \tag{8}$$

$$g^{global} = \begin{cases} g^{local,i}, & \text{erf } F\left(g^{local,i}\right) \leq \text{erf } F\left(g^{global}\right) \\ g^{global}, & \text{erf } F\left(g^{local,i}\right) \geq \text{erf } F\left(g^{global}\right) \end{cases} \tag{9}$$

5) Each particle's position and velocity are updated. In order to improve the performance of the basic PSO approach, PSO with inertia weight strategy [30] is chosen to update the position and velocity. So, each particle's position and velocity are updated by,

$$v_K^{gen+1,i} = \omega v_K^{gen,i} + c_1\xi\left(g^{local,i} - g_K^{gen,i}\right) + c_2\eta\left(g^{global} - g_K^{gen,i}\right) \tag{10}$$

$$g_K^{gen+1,i} = g_K^{gen,i} + v_K^{gen+1,i} \tag{11}$$

These two equations are the core steps of PSHIO. (10) shows that each particle's new velocity consists of three terms. The first term represents each particle's previous velocity influencing on its new velocity. The second term represents each particle's private thinking, usually called 'cognition' section. And the last term represents the group's cooperation, usually called 'social' section. ω is the inertia weight and decreases linearly from 1 to 0.1 as the generation goes in PSHIO. At the beginning, the large inertia weight reduces erf F quickly. Later, the small inertia weight enables precise searching in the solution space [31]. c_1 is a parameter to weight individual best known position, and c_2 is a parameter to weight the group's best known position. c_1 and c_2 are both set to 2, which makes the 'cognition' and 'social' sections to be 1 on average, respectively. ξ and η are uniformly distributed random number in the range $[0, 1]$. Stochastic perturbations and position information exchange take place among these three terms and yield new velocity for each particle. Each particle is moved to a new position through (11).

6) After the first generation reconstructions have been obtained, steps (ii)-(v) are repeated for the next generation.

3. Numerical Experiments

A comparison of HIO, GHIO and PSHIO procedures are given in Fig. 2. Furthermore, we performed a numerical simulation on an example image [see Fig. 3(a)] to demonstrate the difference among images reconstructed by HIO, GHIO and PSHIO. We used the Fourier transform magnitudes of the original image as the measured magnitudes. It is worth mentioning that the PSHIO algorithm can be used to retrieve the Fourier phase of complex-valued or pure phase objects according to phase retrieval theory [32], [33].

Three random particles were generated as the initial particles. For HIO, 175 iterations were performed for each initial particle. β was typically set to 0.7 [16]. GHIO and PSHIO also performed 175 iterations, which consisted of 5 generations, each generation having 35 iterations. It is worth mentioning that different generations and iterations yield different solutions [34]–[36], however, to choose the optimal configuration is not in the scope of this work. The images reconstructed by HIO, GHIO and PSHIO are shown as Fig. 3(b)–(j). The mean-square errors (MSE) of the reconstructed images with respect to the original image are computed and listed below the corresponding images as [37],

$$MSE = \frac{1}{MN}\sum_{m,n=1}^{M,N}\left(g_k(m,n) - g_o(m,n)\right)^2 \tag{12}$$

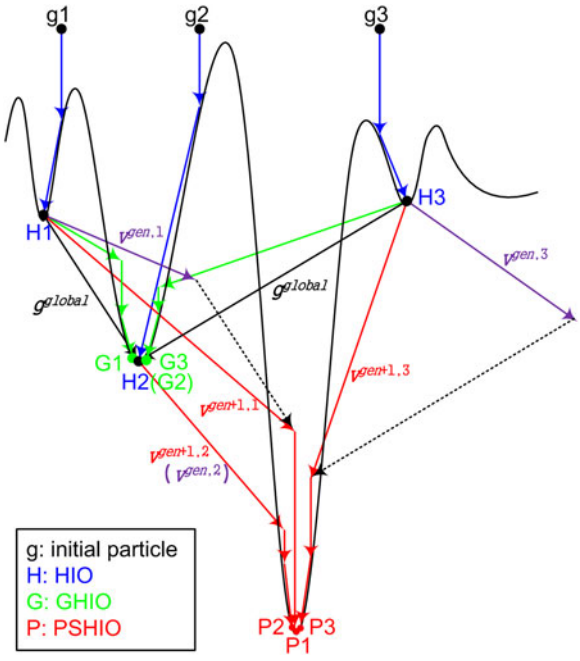

Fig. 2. Comparison of HIO, GHIO, and PSHIO procedures (Colored online). The black curve represents the erf F. Three randomly initial particles g^1, g^2 and g^3 are optimized to local solutions H1, H2 and H3 respectively by HIO (blue lines). With GHIO (green lines), geometric average are performed and H1 and H3 are guided to G1 and G3, which are similar to H2. In the proposed PSHIO (red lines), purple lines represent the velocity vector of each particle and black arrows represent direction vector of each particle from the particle's own best known position to the group's best known position. Composed by the vectors, the new velocities enable the particles to escape from local minima to new positions with lower erf F and to be optimized to a global minimum.

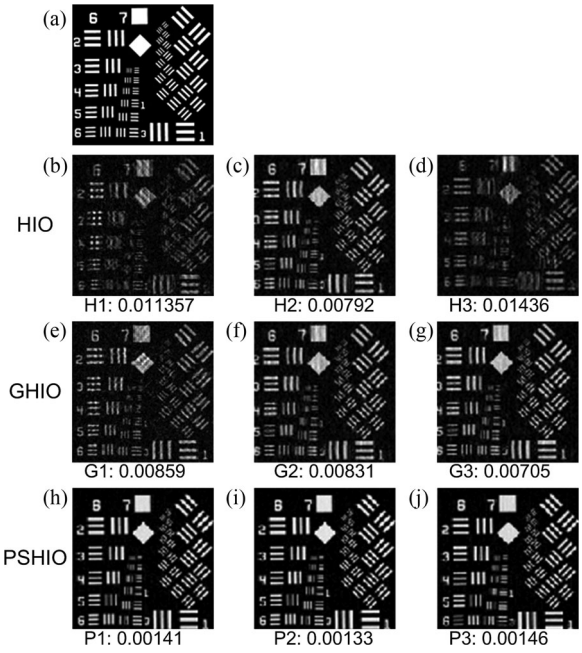

Fig. 3. Comparison of reconstructed images. (a) Original image. (b)–(d) Images reconstructed by HIO. (e)–(g) Images reconstructed by GHIO. (h)–(j) Images reconstructed by PSHIO. The MSE of each reconstructed image is provided below the image.

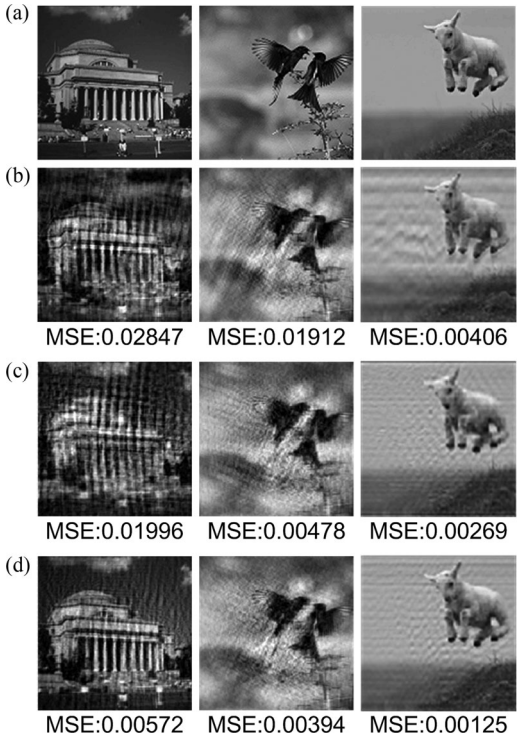

Fig. 4. The comparison of three examples of the set and their reconstructed images. Group (a): original images. Group (b): Reconstructed images by using HIO. Group (c): Reconstructed images by using GHIO. Group (d): Reconstructed images by using PSHIO. The averaged MSE is provided below the averaged reconstructed image.

where M and N are the dimensions of the image. $g_k(m, n)$ and $g_o(m, n)$ are the intensities at the pixel (m, n) of reconstructed and original images, respectively.

The images reconstructed by HIO [see Fig. 3(b)–(d)] have different MSEs from each other, because different initial particles are trapped in different local minima of the solution space. Compared with HIO, the three images yielded by GHIO [see Fig. 3(e)–(g)] have similar MSEs due to its guiding procedure. However, it still suffers from local minima. It is worth mentioning that all MSEs of GHIO yielded images are similar but not equal to that of H2. It is because in GHIO all particles will be geometric averaged by other particles, if no one particle always had the smallest error function value, and therefore no particle can be optimized to the exact same solution as in HIO. Images obtained by PSHIO are shown as Fig. 3(h)–(j). Compared to HIO and GHIO, PSHIO yields images with the lowest MSE due to its capability to escape local minima by stochastic perturbations and information exchange among particles' local solutions.

We further implemented numerical experiments with a group of 35 general images. Six random particles were generated as the initial particles for all three algorithms. Similarly, for HIO, 1000 iterations were performed for each initial particle. For GHIO and PSHIO, optimizations with 25 generations, each generation having 40 iterations, were performed. Three examples of the set and their averaged reconstructed images by using threes algorithms are shown in Fig. 4. The averaged MSE is provided below the averaged reconstructed image.

Fig. 5 shows three averaged MSEs of the 35 reconstructed images as a function of iteration number of the three algorithms. As iteration number increases, the quality of the reconstructed images is improved. It is worth mentioning that even with the same optimization procedure, different objects can leads to dramatically different qualities of the reconstruction. The averaged MSEs in Fig. 5 are presented to demonstrate its statistical property. As iteration number increased, the fitness function erf F became lower and consequently the quality of the reconstructed image was

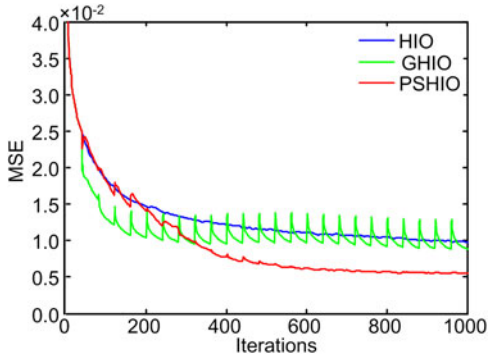

Fig. 5. Averaged MSEs as a function of the iteration number.

improved. The results demonstrated that in this instance of the proposed PSHIO phase retrieval scheme, the assumption that the smaller erf F is, the better quality the reconstructed image of the current particle has.

The MSEs of the three algorithms are equal during the first generation reconstruction procedure. Because the first generation of both GHIO and PSHIO are run based on HIO with the same random initial particle. Specifically, we made the following observations:

1) MSE line yielded by HIO converges at a larger value than those of GHIO and PSHIO, as a result of being trapped in local minima after several hundred iterations.
2) MSE line yielded by GHIO converges faster than both HIO and PSHIO because the particle with the smallest error function value in the previous generation is always used to guide other particles in the next generation. However, the reconstructed images experience an oscillation in quality after its MSE converges to a certain value. It happens due to the geometric average operation at the end of each generation which obtains particles with larger error function value as the initial particles for the next generation. Eventually, GHIO converges to similar MSE value to that of HIO because both algorithms lack the ability to escape the local minima once they are trapped.
3) MSE line yielded by PSHIO converges at a smaller value than both HIO and GHIO, because of its increased possibility of reaching global minimum by stochastic perturbations and information exchange among particles. However, it converges slower than GHIO because the stochastic perturbation also induces extra randomness which will slow the searching progress.
4) After 1000 iterations, the averaged MSEs of HIO, GHIO and PSHIO are 0.0098, 0.0087 and 0.0055, respectively. The averaged MSE of the images reconstructed by PSHIO is 43.88% and 36.78% smaller than those of the images reconstructed by HIO and GHIO, demonstrating PSHIO's feasibility of increasing the possibility to reach global minimum in phase retrieval optimization.

Fig. 6 showed images reconstructed from the experimentally obtained Fourier magnitude of a transmissive object [see Fig. 6(a)]. The Fourier magnitude of the object [see Fig. 6(b)] was obtained using correlation of light intensity fluctuation, i.e., the Hanbury Brown and Twiss correlation [38]. Fig. 6(c)–(e) showed three groups of images reconstructed by HIO, GHIO, and PSHIO, respectively. In fact, we randomly generated six initial particles for the phase retrieval process but illustrated only three of them for each approach. Because the object is a simple one, three of six particles led to acceptable reconstructions by HIO. However, in Fig. 6, we deliberately chose the low quality ones for HIO to show that the initial position influenced the reconstruction dramatically, and for GHIO the low quality particles could jeopardize the particles with better qualities. In contrary, for PSHIO, all six particles yielded relatively good reconstructions, showing an agreement with the numerical simulation, as well as demonstrating the feasibility of the proposed PSHIO.

It is worth mentioning that the method can be limited due to three aspects. First, PSO is a stochastic global optimization, it increases the possibility of finding the global minimum, but does

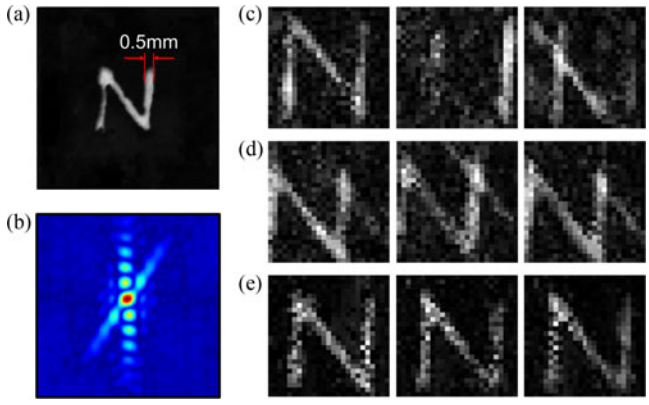

Fig. 6. Experiment results. (a) A photograph of the transmissive object. (b) The Fourier magnitude of the object obtained using intensity fluctuation correlation. (c)–(e) Three groups of images reconstructed by HIO, GHIO, and PSHIO, respectively.

not always guarantee it can be found. Second, the effectiveness of the method is also influenced by non-convexity level of the phase retrieval optimization problem [23], [39], [40] i.e., the different objects. The higher the non-convexity level is, the less possible the method to reach the global minimum. Third, a lower erf F function value isn't strictly equivalent to a better quality of the reconstructed image [16], [18].

Also, we recently realized that the reconstructed images can be improved by multiple captures which provide constrains for each other, such as ptychography and Fourier ptychography [41]. We think that by retrieving better phases, our proposed PSHIO method can be further utilized in ptychography to yield better result.

4. Conclusion

In this work, we proposed a phase retrieval scheme by adopting PSO to HIO, termed as PSHIO. Taking advantage of PSO's stochastic global optimization, the solutions of HIO are moved from local minima to global minimum. A group of general images are used to verify the feasibility of this scheme. Numerical experiments demonstrated that PSHIO retrieves more accurate phase information, and consequently reconstructs images with better qualities, compared to HIO and GHIO. The averaged MSE of 35 images reconstructed by PSHIO is respectively 43.88% and 36.78% smaller than those of the images reconstructed by HIO and GHIO. The feasibility of PSHIO was demonstrated by the results from actual experiments, which showed an agreement with the simulation. Our proposed PSHIO scheme increases the possibility of reaching the global minimum in phase retrieval optimization, and therefore can be applied to Fourier spectrum based image recovery techniques.

References

[1] J. Rosenblatt, "Phase retrieval," *Commun. Math. Phys.*, vol. 95, no. 3, pp. 317–343, Sep. 1984.
[2] G. Z. Yang, B. Z. Dong, B. Y. Gu, J. Y. Zhuang, and O. K. Ersoy, "Gerchberg-saxton and Yang-Gu algorithms for phase retrieval in a nonunitary transform system: A comparison," *Appl. Opt.*, vol. 33, no. 2, pp. 209–218, Jan. 1994.
[3] D. S. Early and D. G. Long, "Image reconstruction and enhanced resolution imaging from irregular samples," *IEEE Trans. Geosci. Remote Sens.*, vol. 39, no. 2, pp. 291–302, Feb. 2001.
[4] Y. Zhang, G. Pedrini, W. Osten, and H. Tiziani, "Whole optical wave field reconstruction from double or multi in-line holograms by phase retrieval algorithm," *Opt. Exp.*, vol. 11, no. 24, pp. 3234–3241, Dec. 2003.
[5] M. Jiang and G. Wang, "Convergence studies on iterative algorithms for image reconstruction," *IEEE Trans. Med. Imag.*, vol. 22, no. 5, pp. 569–579, Jun. 2003.
[6] M. He, X. Y. Xu, and Z. Liu, "Image reconstruction algorithms in electromagnetic tomography," in *Proc. 8th Int. Conf. IEEE Signal Process.*, 2006, pp. 16–20.

[7] G. R. Ying, Q. Wei, X. Shen, and S.S Han, "A two-step phase-retrieval method in Fourier-transform ghost imaging," *Opt. Commun.*, vol. 281, no. 5, pp. 5130–5132, Jul. 2008.
[8] F. Hüe, J. M. Rodenburg, A. M. Maiden, F. Sweeney, and P. A. Midgley, "Wave-front phase retrieval in transmission electron microscopy via ptychography," *Phys. Rev. B*, vol. 82, no. 82, pp. 7174–7182, Sep. 2010.
[9] J. R. Fienup, "Phase retrieval algorithms: A personal tour [Invited]," *Appl. Opt.*, vol. 52, no. 1, pp.45–56, Jan. 2013.
[10] D. V. Strekalov, I. Kulikov, and N. Yu, "Imaging dark objects with intensity interferometry," *Opt. Exp.*, vol. 22, no. 10, pp. 12339–12348, May 2014.
[11] E. Huuskonen-Snicker, V. A. Mikhnev, and M. K. Olkkonen, "Discrimination of buried objects in impulse GPR using phase retrieval technique," *IEEE Trans. Geosci. Remote Sens.*," vol. 53, no. 2, pp. 1001–1007, Jul. 2014.
[12] J. W. Miao, T. Ishikawa, I. K. Robinson, and M. M. Murnane, "Beyond crystallography: Diffractive imaging using coherent x-ray light sources," *Science*, vol. 348, no. 6234, pp. 530–535, May 2015.
[13] M. J. Sun *et al*., "Single-pixel three-dimensional imaging with time-based depth resolution," *Nat. Commun.*, vol. 7, Jul. 2016, Art. no. 12010.
[14] F. Fogel, I. Waldspurger, and A. D'Aspremont, "Phase retrieval for imaging problems," *Math. Program. Comput.*, vol. 8, no. 3, pp. 1–25, Sep. 2016.
[15] R. W. Gerchberg and W. O. Saxton, "A practical algorithm for the determination of phase from image and diffraction plane pictures," *Optik*, vol. 35, no. 2, pp. 237–246, 1972.
[16] J. R. Fienup, "Phase retrieval algorithms: A comparison," *Appl. Opt.*, vol. 21, no. 15, pp. 2758–2769, Aug. 1982.
[17] V. Elser, "Phase retrieval by iterated projections," *J. Opt. Soc. Amer. A, Opt. Image Sci. Vis.*, vol. 20, no. 1, pp. 40–55, Jan. 2003.
[18] H. H. Bauschke, P. L. Combettes, and D. R. Luke, "Hybrid projection-reflection method for phase retrieval," *J. Opt. Soc. Amer. A, Opt. Image Sci. Vis.*, vol. 20, no. 6, pp. 1025–1034, Jun. 2003.
[19] D. R. Luke and D. Russell, "Relaxed averaged alternating reflections for diffraction imaging," *Inverse Problems*, vol. 21, no. 1, pp. 37–50, Nov. 2004.
[20] H. Shioya and K. Gohara, "Generalized phase retrieval algorithm based on information measures," *Opt. Commun.*, vol. 266, no. 1, pp. 88–93, Apr. 2006.
[21] D. C. Hyland, "Analysis of noise-reducing phase retrieval," *Appl. Opt.*, vol. 55, no. 13, pp. 3493–3501, May 2016.
[22] X. Gao, L. J. Feng, and X. Y. Li, "An improved image reconstruction method for optical intensity correlation Imaging," *Opt. Commun.*, vol. 380, pp. 452–461, Jun. 2016.
[23] S. Marchesini, "Invited article: A [corrected] unified evaluation of iterative projection algorithms for phase retrieval," *Rev. Sci. Instrum.*, vol. 78, no. 1, Apr. 2007, Art. no. 049901.
[24] J. A. Rodriguez, R. Xu, C. C. Chen, Y. Zou, and J. W. Miao, "Oversampling smoothness: An effective algorithm for phase retrieval of noisy diffraction intensities," *J. Appl. Crystallogr.*, vol. 46, no. 2, pp. 312–318, Apr. 2013.
[25] C. C. Chen, J. W. Miao, C. W. Wang, and T. K. Lee, "Application of optimization technique to noncrystalline x-ray diffraction microscopy: Guided hybrid input-output method," *Phys. Rev. B*, vol. 76, no. 76, pp. 3009–3014, Aug. 2007.
[26] Y. Shechtman, Y. C. Eldar, O. Cohen, H. N. Chapman, J. W. Miao, and M. Segev, "Phase retrieval with application to optical imaging: A contemporary overview," *IEEE Signal Process. Mag.*, vol. 32, no. 3, pp. 87–109, Apr. 2015.
[27] J. Kennedy and R. C. Eberhart, "Particle swarm optimization," in *Proc. Int. Conf. IEEE Neural Netw.*, 2002, pp. 1942–1948.
[28] S. Baskar, R. T. Zheng, A. Alphones, N. Q. Ngo, and P. N. Suganthan, "Particle swarm optimization for the design of low-dispersion fiber Bragg gratings," *IEEE Photon. Technol. Lett.*, vol. 17, no. 3, pp. 615–617, Feb. 2005.
[29] P. G. Zhang, C. L. Yang, Z. H. Xu, Z. L. Cao, Q. Q. Mu, and L. Xuan, "Hybrid particle swarm global optimization algorithm for phase diversity phase retrieval," *Opt. Exp.*, vol. 24, no. 22, pp. 25704–25717, Oct. 2016.
[30] Y. Shi and R. C. Eberhart, "A modified particle swarm optimizer," in *Proc. Int. Conf. IEEE Evol. Comput.*, 1998, pp. 439–439.
[31] Y. Shi and R. C. Eberhart, "Parameter selection in particle swarm optimization," in *Proc. Int. Conf. IEEE Evol. Program.*, 1998, pp. 591–600.
[32] A. M. Kowalczyk and J. R. Fienup, "Phase retrieval for a complex-valued object by using a low-resolution image," *J. Opt. Soc. Amer. A, Opt. Image Sci. Vis.*, vol. 7, no. 3, pp. 450–458, Mar. 1990.
[33] W. Mcbride, N. L. O'Leary, and L. J. Allen, "Retrieval of a complex-valued object from its diffraction pattern," *Phys. Rev. Lett.*, vol. 93, no. 23, Dec. 2004, Art. no. 233902.
[34] C. Y. Song *et al*., "Nanoscale imaging of buried structures with elemental specificity using resonant x-ray diffraction microscopy," *Phys. Rev. Lett.*, vol. 100, no. 2, Jan. 2008, Art. no. 025504.
[35] R. Dronyak *et al*., "Electron diffractive imaging of nano-objects using a guided method with a dynamic support," *Appl. Phys. Lett.*, vol. 95, no. 11, Sep. 2009, Art. no. 161911.
[36] T. Y. Lan, P. N. Li, and T. K. Lee, "Method to enhance the resolution of x-ray coherent diffraction imaging for non-crystalline bio-samples," *New J. Phys.*, vol. 16, no. 3, Mar. 2014, Art. no. 033016.
[37] M. J. Sun, X. D. He, M. F. Li, and L. A. Wu, "Thermal light subwavelength diffraction using positive and negative correlations," *Chin. Opt. Lett.*, vol. 14, no. 4, Apr. 2016, Art. no. 040301.
[38] R. Hanbury Brown and R. Q. Twiss, "Interferometry of the intensity fluctuation in light II. An experimental test of the theory for partially coherent light," *Proc. Roy. Soc. London A, Math. Phys. Sci.*, vol. 243, no. 1234, pp. 291–319, 1958.
[39] A. Levi and H. Stark, "Image restoration by the method of generalized projections with application to restoration from magnitude," in *Proc. Int. Conf. IEEE Acoust., Speech, Signal Process.*, 1984, pp. 88–91.
[40] H. H. Bauschke, P. L. Combettes, and D. R. Luke, "Phase retrieval, error reduction algorithm, and Fienup variants: A view from convex optimization," *J. Opt. Soc. Amer. A, Opt. Image Sci. Vis.*, vol. 19, no. 7, pp. 1334–1345, Jul. 2002.
[41] A. P. Konijnenberg, W. M. J. Coene, S. F. Pereira, and H. P. Urbach, "Combining ptychographical algorithms with the hybrid input-output (HIO) algorithm," *Ultramicroscopy*, vol. 171, no. 43, pp. 43–54, Aug. 2016.